

Figure 1. Punching failure perimeter adopted for the evaluation of the punching resistance when columns have: (a) and (b) square cross section, (c) circular cross section.

A MODEL TO SIMULATE THE CONTRIBUTION OF FIBRE REINFORCEMENT FOR THE PUNCHING RESISTANCE OF RC SLABS

Bernardo N. Moraes Neto ¹, Joaquim A.O. Barros ², Guilherme S.S.A. Melo ³

¹ University of Minho/University of Brasília-UnB, Dep. Civil Eng., School of Eng., Guimarães, Portugal, bnmn@hotmail.com.

² University of Minho, ISE, Dep. Civil Eng., School of Eng., Campus de Azurém, Guimarães, Portugal, barros@civil.uminho.pt.

³ University of Brasília-UnB, Dep. Civil Eng., Campus of Darcy Ribeiro, Brasília, Brasil, melog@unb.br.

Abstract

In this paper analytical formulations are developed for the prediction of the punching resistance of flat slabs of steel fibre reinforced concrete (SFRC) flexurally reinforced with steel bars. By performing statistical analysis with a database that collects experimental results on the characterization of the post-cracking behaviour of SFRC, equations are determined for the evaluation of the residual flexural tensile strength parameters (f_{Ri}) from fundamental data that characterize steel fibres. The f_{Ri} strength parameters proposed by CEB-FIP 2010 were used for the definition of the stress-crack width law ($\sigma-w$) that simulates the fibre reinforcement mechanisms in cement based materials. In the second part of the paper is described an

23 analytical formulation based on the concepts proposed by Muttoni and Ruiz, where the σ -w law is
24 conveniently integrated for the simulation of the contribution of steel fibres for the punching resistance of
25 SFRC slabs. By using a database composed of 154 punching tests with SFRC slabs, the good predictive
26 performance of the developed proposal is demonstrated. The good performance of this model is also
27 evidenced by comparing its predictions to those from other models.

28

29 **Keywords:** Reinforced concrete, Flat slab, Punching, Steel fibre reinforced concrete, Analytical models.

30

31 **INTRODUCTION**

32 Recent experimental programs have shown the possibility of building structural systems based on flat slabs
33 of steel fibre reinforced concrete (SFRC) supported on reinforced concrete (RC) columns (Espion 2004;
34 Mandl 2008; Destrée *et al.* 2009; Destrée and Mandl 2008; Barros *et al.* 2012). This type of slabs is
35 generally designated by Elevated Steel Fibre Reinforced Concrete Slabs (ESFRC), and it includes a
36 minimum continuity rebars, also referred as anti-progressive collapse rebars, placed in the bottom of the slab
37 in the alignment of the columns (Sasani and Sagioglu 2008). The results obtained in these experimental tests
38 have demonstrated that this construction system fulfills the structural exigencies required for residential
39 buildings, and is a competitive alternative to the available conventional construction methods. However, a
40 reliable acceptance of this innovative construction system also requires the existence of design guidelines
41 that can predict its structural behaviour with high accuracy, namely the punching resistance, since punching
42 failure is quite brittle and, in general, conducts to the global collapse of a building (Gardner *et al.* 2002).

43 In terms of punching resistance of conventionally reinforced concrete flat slabs, in general, the actual design
44 standards, such is the case of ACI 318 (2008), BS 8110 (1985), EC2 (2004), and CEB-FIP Model Code
45 1990, adopt the approach that the ultimate punching resistance, $V_{R,d}$, is obtained adding the parcel due to the
46 concrete resistance, $V_{R,cd}$, to the term that simulates the contribution of shear reinforcement, $V_{R,sd}$, e.g.,
47 $V_{R,d}=V_{R,cd}+V_{R,sd}$. For slabs without shear reinforcement, $V_{R,d}=V_{R,cd}$, and the design procedure for punching is
48 based on the verification that the nominal shear stress, $v_{N,d}$, in two or more critical sections around the
49 column does not exceed the nominal shear strength, $v_{R,d}$, e.g., $v_{R,d}\geq v_{N,d}$.

50 Recently, the CEB-FIP Model Code 2010 proposed recommendations for the evaluation of the flexural and
51 shear resistance of members made by fibre reinforced concrete (FRC). These recommendations are
52 supported on residual flexural tensile strength parameters, f_{Ri} , that characterize the post-cracking behaviour
53 of FRC, and are determined from three point bending tests with notched FRC beams. The full definition and
54 the strategy to obtain f_{Ri} from experimental tests, as well as the aforementioned recommendations, are
55 described in the following sections. The CEB-FIP Model Code 2010 has also proposed a very simple
56 approach to simulate the contribution of fibre reinforcement for the punching resistance of FRC flat slabs,
57 $V_{R,fd}$. Several studies have been done with the purpose of developing a design approach for the prediction of
58 the contribution of fibre reinforcement for the punching resistance of SFRC slabs (Narayanan and Darwish
59 1987; Harajli *et al.* 1995; Muttoni and Ruiz 2010; Michels *et al.* 2012), but the predictive performance of
60 these models is generally limited to a relatively small number of punching tests, and the contribution of fibre
61 reinforcement is not based on the most recent knowledge about modelling the post-cracking behaviour of this
62 composite.

63

64 In the present paper a design formulation is proposed for the evaluation of the punching resistance of SFRC
65 slabs. This model is based on the principles proposed by Muttoni and Ruiz (2010), where a stress-crack
66 width relationship is used to simulate the contribution of the fibre reinforcement mechanisms for the
67 punching resistance of SFRC flat slabs, $V_{R,f}$. The $V_{R,f}$ is determined from the f_{Ri} parameters proposed by CEB-
68 FIP Model Code 2010.

69

70 **DESIGN FORMULATIONS PROPOSED BY STANDARD CODES**

71 **Design formulation for flat slabs only reinforced with conventional steel bars**

72 **ACI 318 (2008)**

73 According to ACI 318, the punching resistance of the type of slabs analysed in the present paper is obtained
74 from:

$$\phi \cdot V_{R,d} \geq V_{S,d} \quad (1)$$

75

76 where,

$$V_{R,d} = v_{R,d} \cdot b_0 \cdot d \quad (2)$$

77

78 with

$$v_{R,d} = \min \left[\frac{\sqrt{f_c}}{6} \cdot \left(1 + \frac{2}{\beta_c} \right); \frac{\sqrt{f_c}}{6} \cdot \left(\frac{6 \cdot \alpha_s \cdot d}{b_0} + 1 \right); \frac{\sqrt{f_c}}{3} \right] \quad [\text{MPa}, \text{mm}] \quad (3)$$

79

80 In Eq. (2) b_0 is the perimeter corresponding to the formation of the punching failure surface, assumed
 81 localized at a distance $\alpha=0.5$ from the external face of the column, and with the geometric configuration
 82 represented in Figure 1a. In Eq. (3) β_c is the ratio between the larger and the smaller edge of the column's
 83 cross section, $\alpha_s=3.32$ for columns located in the interior of the building (assumed centrally loaded), such
 84 is the case treated in the present work, f_c is the average concrete compressive strength evaluated using
 85 cylinder specimens, and d is the internal arm of the longitudinal tensile reinforcement of the slab's cross
 86 section.

87

88 **CEB-FIP MODEL CODE 1990**

89 The CEB-FIP Model Code 1990 recommends that the punching resistance of a RC slab without shear
 90 reinforcement should be determined from the following equation:

$$V_{R,d} = v_{R,d} \cdot u_1 \cdot d \quad [\text{MPa}, \text{mm}] \quad (4)$$

91

92 with

$$v_{R,d} = 0.12 \cdot \xi \cdot (100 \cdot \rho \cdot f_c)^{1/3} \quad [\text{MPa}, \text{mm}] \quad (5)$$

93

94 where

$$\xi = 1 + \sqrt{\frac{200}{d}} \quad [\text{mm}]; \quad (6)$$

$$\rho = \sqrt{\rho_x \cdot \rho_y} \quad (7)$$

95

96 The ξ parameter in Eq. (6) aims to simulate the size effect. The reinforcement ratio of the tensile flexural
 97 reinforcement, ρ , is calculated from Eq. (7) by considering the reinforcement ratio ρ_x and ρ_y in the two main
 98 orthogonal directions (x and y). For the evaluation of ρ_x and ρ_y , a width of the slab cross section equal to

99 $e+6\cdot d$ (for the columns of square cross section), or equal to $2\cdot r_c+6\cdot d$ (for the columns of circular cross
 100 section), is considered, Figure 1.

101

102 **EC2 (2004)**

103 In the Eurocode 2, EC2, it is assumed that the punching resistance of RC slabs without shear reinforcement
 104 can be estimated by the following equation:

$$V_{R,d} = v_{R,d} \cdot u_1 \cdot d \quad (8)$$

105

106 with

$$v_{R,d} = \max \left[C_{Rd,c} \cdot k \cdot (100 \cdot \rho \cdot f_c)^{1/3}; 0.035 \cdot k^{3/2} \cdot f_c^{1/2} \right] \quad [\text{MPa, mm}] \quad (9)$$

107

108 where k is defined as ζ (Eq. (6)), but a maximum limit of 2.0 is imposed to k , while ρ is obtained from Eq.
 109 (7) with an upper limit of 0.02. In Eq. (8) the critical perimeter, u_1 , is localized at $2d$ from the external
 110 surface of the column ($\alpha=2$), and can assume the configurations represented in Figures 1b and 1c. In Eq. (9)

$$111 \quad C_{Rd,c} = 0.18/\gamma_c.$$

112

113 **CEB-FIP Model Code 2010**

114 According to the CEB-FIP Model Code 2010, the punching resistance of RC slabs without shear
 115 reinforcement, $V_{R,d} = V_{R,cd}$, is determined from the following equation:

$$V_{R,d} = V_{R,cd} = k_\psi \cdot \frac{\sqrt{f_c}}{\gamma_c} \cdot b_0 \cdot d \quad [\text{MPa, mm}] \quad (10)$$

116

117 where b_0 is the critical punching perimeter at a distance $\alpha=0.5$ from the external surface of the column, as
 118 represented in Figures 1b and 1c. The k_ψ parameter depends of the rotation of the slab, and is determined
 119 from the following equation:

$$k_\psi = \frac{1}{1.5 + 0.9 \cdot \psi \cdot d \cdot k_{dg}} \leq 0.6 \quad [\text{mm}] \quad (11)$$

120

121 where k_{dg} parameter simulates the aggregate interlock:

$$k_{dg} = \frac{32}{16 + d_g} \geq 0.75 \quad [\text{mm}] \quad (12)$$

122

123 being d_g the maximum diameter of the aggregates.

124 The rotation of the slab, ψ , (Figure 2b) required to determine the k_ψ parameter, is evaluated according to the
 125 approach II indicated in CEB-FIP Model Code 2010, by applying the following equation:

$$\psi = 1.5 \cdot \frac{r_s}{d} \cdot \frac{f_{yd}}{E_s} \cdot \left(\frac{m_{sd}}{m_{Rd}} \right)^{1.5} \quad (13)$$

126

127 where r_s indicates the position, in relation to the axis of the column, at which the radial bending moment, m_r ,
 128 is null (Figure 2a). The value of r_s can be considered equal to $0.22 \cdot L_s$ (L_s is replaced by $L_{s,x}$ for the analysis in
 129 x direction, and L_s is replaced by $L_{s,y}$ for the analysis in y direction, Figure 2c) in slabs where the $L_{s,x}/L_{s,y}$ ratio
 130 pertains to the interval $[0.5 - 2.0]$. In Eq. (13) the $m_{sd} = V_{s,d}/8$ (Johansen 1962) and m_{Rd} represents the design
 131 value of the actuating and resisting bending moment, respectively. Both m_{sd} and m_{Rd} are evaluated for a slab
 132 strip of a width of $b_s = 1.5 \cdot (r_{s,x} \cdot r_{s,y})^{0.5} \leq L_{s,min}$, where $r_{s,x}$ and $r_{s,y}$ is the r_s in x and y direction, respectively, and
 133 $L_{s,min}$ is the minimum value between $L_{s,x}$ and $L_{s,y}$, Figure 2c. The strategy to evaluate m_{Rd} will be discussed in a
 134 posterior section.

135

136 **Design formulation for FRC flat slabs flexurally reinforced with conventional steel bars - CEB-FIP**
 137 **Model Code 2010**

138 For SFRC slabs, the CEB-FIP Model Code 2010 recommends the following equation for the evaluation of
 139 the punching resistance:

$$V_{R,d} = V_{R,cd} + V_{R,fd} \quad (14)$$

140

141 where $V_{R,cd}$ is calculated according to Eq. (10), and the parcel corresponding to the contribution of fibre
 142 reinforcement, $V_{R,fd}$, is evaluated from:

$$V_{R,fd} = \frac{f_{Ftk}}{\gamma_F} \cdot b_0 \cdot d \quad (15)$$

143

144 being,

$$f_{Ftu} = f_{Fts} - \frac{w_u}{2.5} \cdot (f_{Fts} - 0.5 \cdot f_{R3} + 0.2 \cdot f_{R1}) \geq 0; \quad f_{Fts} = 0.45 \cdot f_{R1} \quad (16)$$

145

146 In Eq. (15) f_{Ftuk} represents the characteristic value of the ultimate residual flexural tensile strength, which is
 147 calculated for an ultimate crack width (w_u) of 1.5 mm. When the SFRC slab also includes conventional
 148 flexural reinforcement, the CEB-FIP Model Code 2010 suggests the use of $w_u = \psi d/6$, where ψ is calculated
 149 from Eq. (13). The f_{Fts} in Eq. (16) represents the residual flexural tensile strength for the verifications of
 150 serviceability limit states. The f_{Ri} ($i=1$ and 3) parameters indicated in Eq. (16) represent the residual flexural
 151 tensile strength parameters of FRC, and are determined from the load versus Crack Mouth Opening
 152 Displacement ($CMOD$) registered in three point notched beam bending tests, by applying the following
 153 equation:

$$f_{Ri} = \frac{3 \cdot F_{Ri} \cdot L}{2 \cdot b \cdot h_{sp}^2} \quad (17)$$

154

155 where F_{Ri} is the force corresponding to $CMOD_i$, and L (500 mm), b (150 mm) and h_{sp} (125 mm) are the free
 156 span, the width of the cross section and the distance from the tip of the notch to the top surface of the beam,
 157 respectively (CEB-FIP Model Code 2010).

158

159 ASSESSMENT OF THE PREDICTIVE PERFORMANCE OF DESIGN FORMULATIONS 160 PROPOSED BY STANDARD CODES

161 Introduction

162 The predictive performance of the the formulations proposed by standard codes, described in a previous
 163 Section, is evaluated in terms of the $\lambda = V_{exp}/V_{the}$ parameter, where V_{exp} is the punching failure load registered
 164 experimentally, and $V_{the} = V_R = V_{R,c}$ is the punching failure load estimated according to the analytical
 165 formulations of the considered standard codes. The purpose of this section is to determine the formulation
 166 that best predicts the punching failure load of RC flat slabs ($V_R = V_{R,c}$), in order to be adopted with the model
 167 proposed in the present work to estimate the failure load of SFRC flat slabs that are also flexurally reinforced
 168 with steel bars, e.g. $V_{the} = V_R = V_{R,c} + V_{R,f}$. This assessment was executed by considering a database of punching
 169 tests with flat slabs described in the following section.

170

171 **Database (DB)**

172 A database (DB) composed by 154 slabs submitted to punching test configuration was built, 137 of them
173 were reinforced with longitudinal steel bars/grids in order to avoid the occurrence of flexural failure mode.
174 None of these slabs has conventional shear/punching reinforcement. However, 105 slabs composing the DB
175 were made by SFRC. In terms of concrete compressive strength, f_{cm} , the DB is composed of slabs with f_{cm} in
176 the range of 14 to 93 MPa, so a quite high interval exists for a parameter that has a relevant impact on the
177 punching resistance of concrete slabs. For the slabs that were flexurally reinforced with steel bars, the
178 internal arm of this reinforcement (d , Figure 2) has varied from 13 mm to 180 mm, while the reinforcement
179 ratio (ρ) is in the interval 0.4 to 2.75%. In the SFRC slabs, “hooked”, “twisted”, “crimped”, “corrugated”,
180 “paddle” and other types of fibres were used, with an aspect-ratio that varied from 20 to 100, and in a
181 volume percentage $\leq 2\%$. In some of the SFRC slabs (6 specimens), the SFRC was only applied in a region
182 around the loaded area (that represents the position of the column), considered the region where punching
183 failure could occur. In terms of loading conditions, all the slabs of the DB were submitted to a load
184 distributed in a certain area of the slab without transferring any bending moments from the loading device to
185 the slab. In the tests of the DB, the columns were simulated by a RC element monolithically connected to the
186 slab or applying steel plates, or even introducing a semi-spherical device in between the piston of the
187 actuator and the tested slab. The cross section of the columns and steel plates was square or circular. To
188 avoid results that can compromise the reliability of this statistical analysis, the slabs with a thickness lower
189 than 80 mm were discarded, since an eventual influence of size effect can have a detrimental consequence on
190 this study. Furthermore, the slabs where the concrete compressive strength has decreased more than 15% in
191 consequence of the addition of fibres were also neglected, since this decrease reveals that the SFRC mix
192 composition was not properly designed. Further details about the DB can be found elsewhere (Moraes Neto
193 2013).

194 In this section, slabs only reinforced with steel bars are considered for the assessment of the predictive
195 performance of the formulations proposed by standard codes, described in the previous chapter.

196

197 **General statistical analysis procedures**

198 The performance of the formulations proposed by the considered standard codes for the prediction of the
 199 punching resistance of RC slabs is appraised using the collected data registered in the DB. For each proposal,
 200 the obtained values of V_{the} are compared with V_{exp} and a λ factor corresponding to the V_{exp}/V_{the} ratio is
 201 evaluated. The values of λ were classified according to the modified version of the of the *Demerit Points*
 202 *Classification (DPC)* proposed by Collins (2001), where a penalty (PEN) is assigned to each range of λ
 203 parameter according to Table 1, and the total of penalties (Total PEN) determines the performance of the
 204 proposal. The penalty is a weighting factor determined from statistical analysis that takes into account safety,
 205 accuracy and economic aspects (Collins 2001). According to this strategy, the proposal with the minimum
 206 total of penalties is the best one under this framework.

207 In next section the models in analysis are designated as *MODi* ($i=1$ up to 4), with the corresponding
 208 formulation assigned in the footnote of Table 2.

209 In the analysis performed, unit value was assumed for all the safety factors (such is the case of γ_c and γ_F in
 210 equations (10) and (15), respectively) considered by the formulations, and average values were adopted for
 211 the properties of the materials (such as: f_c , f_{ct} , f_{R1} , f_{R3} , f_{Fts} , f_{Ftu}), since the analytical predictions will be
 212 compared to the experimental results. Furthermore, in the evaluation of Eq. (10) of the model proposed by
 213 CEB-FIP Model Code 2010, the Eqs. (11) and (12) that define the punching failure criterion are replaced by
 214 the following ones:

$$k_{\psi} = \frac{3/4}{1 + \psi \cdot d \cdot k_{dg}} \quad [\text{rad, mm}] \quad (18)$$

$$k_{dg} = \frac{15}{16 + d_g} \quad [\text{mm}] \quad (19)$$

215
 216 in order to take into account that average values are now considered (Muttoni 2008).

217
 218 **Results**

219 The results presented in the present section assess the performance of the formulations described in Section
 220 “Design formulation for flat slabs only reinforced with conventional steel bars” for the prediction of the
 221 punching failure load of flat slabs only reinforced with longitudinal bars, e.g. $V_{the}=V_R=V_{R,c}$. The results are
 222 presented in Table 2, and from the analysis it can be concluded that MOD4, corresponding to the one
 223 proposed by CEB-FIP Model Code 2010, has best predicted the punching failure load registered

224 experimentally, with the lowest COV. Furthermore, it is the one with the largest number of predictions in the
225 appropriate safety interval according to the DPC (Table 1), e.g. 21 samples with $\lambda \in [0.85-1.15]$. Therefore, it
226 will be selected for the evaluation of the $V_{R,c}$ in the context of the formulation to be developed for the
227 prediction of the punching failure model of SFRC flat slabs flexurally reinforced with steel bars, Eq. (14).

228

229 **PRACTICAL PROPOSAL FOR THE ESTIMATION OF THE RESIDUAL FLEXURAL TENSILE** 230 **STRENGTH PARAMETERS, f_{Ri}**

231 **Introduction**

232 The predictive performance of the model proposed in the present work for the evaluation of the punching
233 failure load of SFRC flat slabs will be assessed by comparing the estimated results with those available in the
234 DB described in Section “Database (CB)”. As already indicated, the contribution of fibre reinforcement for
235 the punching resistance is simulated by using the concept f_{Ri} , however, these values are not available in the
236 majority of the works composing the DB. Therefore, to apply the proposed model to the tests composing the
237 DB, another database was built by collecting results (f_{Ri}) of the characterization of the post-cracking flexural
238 behaviour of SFRC according to the recommendations of CEB-FIP Model Code 2010. Since the fibre
239 volume percentage, V_f , and fibre aspect ratio, (l_f/d_f), (quotient between fibre length, l_f , and fibre diameter, d_f)
240 are practically the unique common information available in the works forming the DB of the punching tests,
241 the statistical analysis performed with the collected data for the characterization of the post-cracking
242 behaviour of SFRC was governed by the criterion of deriving equations for the f_{Ri} dependent on the V_f and
243 l_f/d_f . The authors are aware that this is a quite simple approach to simulate the fibre reinforcement
244 mechanisms, since other variables like the fibre-matrix bond strength, fibre inclination and fibre embedment
245 length influence the values of f_{Ri} (Cunha *et al.* 2010), but this information is not available in those works.
246 Therefore, a relatively large scatter of results is naturally expected for the relationships $f_{Ri}(V_f, l_f/d_f)$, but
247 actually this is the unique possibility of considering the fibre reinforcement mechanisms according to the
248 CEB-FIP Model Code 2010 for the prediction of the punching failure load of the slabs collected in the DB by
249 applying the proposed model. Preliminary statistical analysis by considering also the bond strength was also
250 carried out (Moraes Neto 2013), but the obtained results have revealed that by also adopting these
251 parameters, the dispersion of the results increase significantly, since a large scatter of bond strength values

252 exists in the bibliography. Taking this into account, the statistical analysis was carried out in order to derive
253 equations that conduct to safe predictions.

254

255 **Database (DB) and procedures for the analysis**

256 A database composed of 69 results from three point notched SFRC beam bending tests was collected
257 (Moraes Neto 2013). The analysis of the DB has indicated that fibre reinforcement index, $V_f \cdot l_f / d_f$, is the most
258 influential parameter on the f_{Ri} values. Taking into account the geometric characteristics and volume
259 percentage of the steel fibres most used in the available experimental programs of punching SFRC slabs, this
260 database is restricted to the tests with concrete reinforced with hooked ends steel fibres, in a volume
261 percentage ranging from 0.13% to 1.25% and with fibre aspect-ratio in the interval 50 to 80.

262 In the first step of the analysis of the information available in the DB, relationships between f_{Ri} and $V_f \cdot l_f / d_f$
263 were established (Moraes Neto 2013). The predictive performance of the equations were then evaluated in
264 terms of the $\lambda_i = f_{Ri,exp} / f_{Ri,the}$ parameter, where $f_{Ri,exp}$ and $f_{Ri,the}$ is, respectively, the residual flexural strength
265 parameter recorded experimentally (available in the DB) and estimated according to the obtained $f_{Ri} - V_f \cdot l_f / d_f$
266 relationships. The predictive performance of these relationships was also appraised by using a modified
267 version of the *DPC*, where a penalty is assigned to each range of λ_i parameter according to Table 1, and the
268 total of penalties determines the performance of the $f_{Ri} - V_f \cdot l_f / d_f$ relationship. To assure stable predictions, the
269 statistical analysis was executed in order to provide average values for $\lambda_{1=f_{R1,exp}/f_{R1,the}}$ and $\lambda_{2,the}$ in the lower
270 bound of the interval considered as “conservative” (Table 1), which assures safe predictions in terms of
271 design philosophy.

272

273 **Assesment of the predictive performance of the $f_{Ri} - V_f \cdot l_f / d_f$ relationship**

274 Analyzing the results of the DB it was realized that the $f_{Ri} - V_f \cdot l_f / d_f$ function that best fit the results is of the
275 type (Moraes Neto 2013), $f_{Ri} = k_j \cdot (V_f \cdot l_f / d_f)^{c_j}$. To derive the k_j and the c_j values ($j=1$ and 2), a
276 parametric analysis was executed (Moraes Neto 2013) in order to obtain the best compromise in terms of the
277 lowest R-squared values (R^2) of the fitting process and the lowest total penalties according to the modified
278 *DPC*, having resulted the following equations:

279

$$f_{R1} = k_1 \cdot \left(V_f \cdot \frac{l_f}{d_f} \right)^{c1} = 7.5 \cdot \left(V_f \cdot \frac{l_f}{d_f} \right)^{0.8} \quad [\text{MPa}] \quad (20)$$

$$f_{R3} = k_2 \cdot \left(V_f \cdot \frac{l_f}{d_f} \right)^{c2} = 6.0 \cdot \left(V_f \cdot \frac{l_f}{d_f} \right)^{0.7} \quad [\text{MPa}] \quad (21)$$

$$f_{R3} = k_3 \cdot f_{R1} = 0.85 \cdot f_{R1} \quad (22)$$

280

281 Eq. (22) shows a tendency for a linear relationship between f_{R1} and f_{R3} , which was already pointed out in a
 282 previous work (Barros *et al.* 2005).

283 The predictive performance of Eqs. (20) and (21) was assessed by taking the results estimated for the λ_i
 284 parameter, and considering the dispersion of the results and total penalties according to the modified *DPC*.

285 The obtained results are presented in Figure 3. A “box and whiskers” plot of the λ ratio for the f_{R1} and f_{R3} is
 286 represented in Figure 3b. The box plot diagram graphically depicts the statistical five-number summary,
 287 consisting of the minimum and maximum values, and the lower (Q1), median (Q2) and upper (Q3) quartiles.

288 Table 3 resumes the obtained results. As expected, a relatively high dispersion was obtained for the
 289 predictions of both parameters, which is intrinsically dependent of the dispersion of results in the DB for the
 290 f_{R1} and f_{R3} , since the values of these parameters are also affected by the properties of the surrounding cement
 291 matrix, but not considered in the present approach due to the reasons already pointed out. The authors are
 292 doing an effort for increasing the database on the characterization of the post-cracking behaviour of SFRC, in
 293 order to derive more reliable equations for the determination of f_{Ri} .

294 In a design context of a SFRC slab, three point notched SFRC beam bending tests should be executed
 295 according to the recommendations of CEB-FIP Model Code 2010 in order to obtain the f_{Ri} of the SFRC, and
 296 these values are directly used in the proposed model for the evaluation of the punching failure load of a
 297 SFRC slab supported on columns.

298

299 **THE CONTRIBUTION OF FIBRE REINFORCEMENT FOR THE PUNCHING RESISTANCE OF** 300 **SFRC FLAT SLABS**

301 The contribution of fibre reinforcement mechanisms for the punching resistance of SFRC flat slabs, $V_{R,f}$, has
 302 been investigated by several researchers (Narayanan and Darwish 1987; Harajli *et al.* 1995; Muttoni and

303 Ruiz 2010; Choi *et al.* 2007; Higashiyama *et al.* 2011), but none of them has acquired generalized
304 conclusions to be considered as design guideline criteria.

305 With the aim of contributing for the development of a formulation that is sufficiently simple to be adopted in
306 the design practice, and with scientific rigour capable of simulating with enough accuracy a phenomena that
307 has a brittle character and huge impact if a collapse occurs (Gardner *et al.* 2002), a new approach to
308 determine $V_{R,f}$ is described in this section by combining the most comprehensible knowledge available. This
309 formulation is based on the principles proposed by Muttoni and Ruiz (2010), being the contribution of fibre
310 reinforcement mechanisms simulated by a stress vs crack width law, $\sigma_f(w)$, recommended by the CEB-FIP
311 Model Code 2010, but considering Eqs. (20) and (21) to determine $\sigma_f(w)$.

312 According to Muttoni and Ruiz (2010), it is acceptable to consider that a slab with axisymmetric structural
313 conditions, when submitted to a load level corresponding to the failure state, can be regarded as a group of
314 radial segments that rotate as rigid bodies, Figure 4.

315 The reinforcement mechanisms offered by the fibres crossing the critical punching surface are simulated by
316 the stress-crack width relationship (Figure 5a), and after convenient integration of $\sigma_f(w)$ at the fracture
317 surface, the fiber reinforcement contribution for the punching resistance $V_{R,f}$ can be obtained.

318 According to the Critical Shear Crack Theory (CSCT) (Muttoni 2008; Muttoni and Schwartz 1991), the
319 crack opening of the punching failure crack, w , is proportional to the rotation of the slab, ψ , and the distance
320 from the bottom surface of the slab, z (Figure 5b):

$$w(\psi, z) = \mu \cdot \psi \cdot z \quad (23)$$

321
322 where μ is the coefficient relating the rotation ψ with the crack opening w . The μ parameter was obtained by
323 using the rotation values at punching failure load, ψ_u , of the slabs composing the database introduced in
324 Section “Database (DB)”. For each slab its ψ_u was evaluated from available experimental data, and assuming
325 that the ultimate crack width, w_u , should be in the interval 1.5 to 3.0 mm, for each w_u in this interval the
326 corresponding value of the μ parameter is determined from Eq. (23). The w_u was determined at the level of
327 the tensile flexural reinforcement, considering $z=d-x$ (Figure 5), where the position of the neutral axis, x , is
328 determined by applying the approach recommended by CEB-FIP Model Code 2010 (Figure 6), where f_{Fu} is
329 obtained from Eq. (16) with $w_u=2.5$ mm, as suggested by this standard. Therefore, for the μ parameter that
330 respect Eq. (23) for the considered w_u , it is obtained the contribution of fibre reinforcement for the punching

331 resistance, $V_{R,f}$, and applying Eq. (14) the punching failure load is estimated and compared to the value
 332 registered experimentally. This algorithm was executed for the adopted interval of w_u , and the pair of w_u and
 333 μ parameters that have best predicted the punching failure load of the experimental programs collected in the
 334 database was $\mu=2.5$ and $w_u=2.5\text{mm}$ (Moraes Neto 2013).

335 According to Moraes Neto (2013) ψ_u is calculated from the following equation:

$$\psi_u = 0.35 \cdot \left(\frac{m_R}{E \cdot I_1} - \chi_{ts} \right) \cdot r_s \quad (24)$$

336

337 where,

$$E \cdot I_1 = \rho \cdot \beta \cdot E_s \cdot d^3 \cdot \left(1 - \frac{x}{d} \right) \cdot \left(1 - \frac{x}{3 \cdot d} \right) \quad (25)$$

338

339 and

$$\chi_{ts} = \frac{f_{ct}}{\rho \cdot \beta \cdot E_s} \cdot \frac{1}{6 \cdot h} \cong 0.5 \cdot \frac{m_{cr}}{E \cdot I_1} \quad (26)$$

340

341 In equation (25), $E \cdot I_1$ represents the flexural stiffness of SFRC cracked cross section, obtained according to
 342 the procedures adopted for RC members (Moraes Neto 2013), and assuming a stabilized cracking stage. The
 343 contribution of fibre reinforcement for the $E \cdot I_1$ is only indirectly taken in the evaluation of the neutral axis, x ,
 344 Figure 6. In Eq. (25) β is a factor to take into account the real arrangement of the reinforcement, since the
 345 CSCT is supported on the principle of axisymmetric structural conditions, but the majority of the built and
 346 tested RC flat slabs have orthogonal distribution of the reinforcement (Guandalini 2005). According to
 347 Muttoni (2008), $\beta=0.6$ yields to satisfactory results. The evaluation of the position of the neutral axis, x , was
 348 made according to the recommendations of CEB-FIP Model Code 2010, see Figure 6.

349 The χ_{ts} factor in Eq. (26) simulates the post-cracking tensile strength of cracked concrete (tension stiffening
 350 effect), where f_{ct} is the concrete tensile strength, E_s is the elasticity modulus of the steel reinforcement, ρ is
 351 the reinforcement ratio of the tensile flexural reinforcement, h is the slab thickness, and $m_{cr} = f_{ct} h^2 / 6$ is the
 352 cracking moment.

353 To evaluate $V_{R,f}$ it is assumed that the post-cracking stress law, $\sigma_f(w) = \sigma_f(\psi, z)$, can be represented by the
 354 following linear constitutive σ - w approach recommended by CEB-FIP Model Code 2010:

$$\sigma_f(w) = f_{Ftu}(w) = f_{Fts} - \frac{w}{2.5} \cdot (f_{Fts} - 0.5 \cdot f_{R3} + 0.2 \cdot f_{R1}) \geq 0 \quad (27)$$

355

356 Replacing Eq. (23) into Eq. (27) yields:

$$\sigma_f(\psi, z) = f_{Fts} - \frac{\mu \cdot \psi \cdot z}{2.5} \cdot (f_{Fts} - 0.5 \cdot f_{R3} + 0.2 \cdot f_{R1}) \geq 0 \quad (28)$$

357

358 The $V_{R,f}$ is obtained by integrating $\sigma_f(\psi, z)$ on the area A_0 , where A_0 , see Figure 5a, represents the horizontal

359 projection of the punching failure surface (Moraes Neto 2013):

$$V_{R,f} = \int_{A_0} \sigma_f(\psi, z) \cdot dA_0 \quad (29)$$

$$V_{R,f}(\psi) = \pi \cdot d \cdot (1 - 2 \cdot k) \cdot \left(2 \cdot \Omega_1 \cdot \Omega_3 + d \cdot \left\{ \Omega_1 \cdot \Omega_4 - \Omega_2 \cdot \Omega_3 \cdot \psi - 2 \cdot d \cdot \Omega_2(\psi) \cdot \Omega_4 \cdot \left[\frac{(1-k) \cdot (1-2 \cdot k + k^2) - k^3}{3 \cdot (1-2 \cdot k)} \right] \right\} \right) \quad (30)$$

360

361 where,

$$\Omega_1 = f_{Fts}; \quad \Omega_2 = \frac{\mu \cdot (f_{Fts} - 0.5 \cdot f_{R3} + 0.2 \cdot f_{R1})}{2.5}; \quad \Omega_3 = r_c; \quad \Omega_4 = \frac{1}{2 \cdot (1-k)} \quad (31)$$

$$\psi = \psi_u = 0.35 \cdot \left(\frac{m_R}{E \cdot I_1} - \chi_{ts} \right) \cdot r_s; \quad k = \frac{x}{d} \quad (32)$$

362

363 To evaluate the $V_{R,f}$ an assumption was assumed by considering $\sigma_f(\psi, z) = \sigma_f(w) = \sigma_f(w_u)$ (see Eq. (23)) and

364 adopting for w_u the value 1.5 mm recommended by CEB-FIP Model Code 2010 (clause 7.7.3.5.3).

365 Therefore:

$$V_{R,f} = \int_{A_0} \sigma_f(\psi, z) \cdot dA_0 = \int_{A_0} \sigma_f(w_u) \cdot dA_0 = \sigma_f(w_u) \cdot A_0 \quad (33)$$

366

367 where $\sigma_f(w_u)$ is obtained from Eq. (16):

$$\sigma_f(w_u) = f_{Ftu}(w_u) = f_{Fts} - \frac{w_u}{2.5} \cdot (f_{Fts} - 0.5 \cdot f_{R3} + 0.2 \cdot f_{R1}) \geq 0 \quad (34)$$

368

369 resulting:

$$V_{R,f} = \left[f_{Fts} - \frac{1.5}{2.5} \cdot (f_{Fts} - 0.5 \cdot f_{R3} + 0.2 \cdot f_{R1}) \right] \cdot A_0 \quad (35)$$

370

371 **ASSESSMENT OF THE PREDICTIVE PERFORMANCE OF FORMULATIONS FOR SFRC FLAT**
372 **SLABS**

373 Since the formulation of CEB-FIP Model Code 2010 has best fitted the $V_{R,c}$ of the collected DB, it was
374 selected to be coupled with the proposed model that predicts the contribution of fibre reinforcement for the
375 punching resistance of SFRC flat slabs, $V_{R,f}$, resulting a model capable of estimating the the punching failure
376 load of SFRC slabs reinforced with longitudinal steel bars: $V_{the}=V_R=V_{R,c}+V_{R,f}$. In the previous Section two
377 equations were proposed to estimate $V_{R,f}$: i) Eq. (30) that requires performing a full integration of the crack
378 opening–fibre stress law, thereby is herein designated as *The-refin*; 2) Eq. (35) that is more simple to obtain,
379 thereby is herein designated as *The-simpl*, where *refin* and *simpl* means refined and simplified, respectively.
380 In Table 4 the predictive performance of these two models is compared to the one resulting from the
381 application of the formulation proposed by CEB-FIP Model Code 2010 that was already described. It can be
382 concluded that both proposed formulations evidence excellent predictive performance with a relatively small
383 COV. Both formulations present average value of λ much closer to the unit value than the CEB-FIP model,
384 and lower COV. Furthermore, these models have also the largest number of predictions in the appropriate
385 safety interval according to the DPC (Table 1). Based on the results and considering its easy attainment, it is
386 recommended to use *The-simpl* approach to predict $V_{R,f}$, based on Eq. (35).

387 The CEB-FIP Model Code 2010 provides a large number of predictions against safety, e.g. a λ value in the
388 interval [0.50-0.85[, considered “Dangerous” according to the DPC (see Table 1), was obtained for 39 slabs.
389 In the CEB-FIP Model Code 2010 a constant post-cracking residual strength is assumed distributed in the
390 punching fracture surface for the simulation of the fibre reinforcement contribution for the punching
391 resistance. This is in fact the same strategy adopted in the simplified approach herein proposed (Eq. (35)),
392 but the relatively high number of unsafe predictions demonstrates that the punching failure surface assumed
393 in this standard (*b₀.d*) seems not realistic, or not compatible with the assumption of a constant residual
394 strength distribution in the punching failure surface. In this model the $V_{R,f}$ is calculated from f_{Fu} determined
395 by Eq. (16). To evaluate f_{Fu} , instead of adopting $w_u=\psi\cdot d/6$ as recommended by this standard, it was assumed
396 $w_u=1.5$ mm, since the former approach lead to more unsafe predictions. If a proper safety criterion is
397 considered as the one that 85% of the samples remains in the interval $\lambda=[0.85-1.15[$, a $w_u\approx 4.0$ mm should be
398 adopted in the model proposed by CEB-FIP Model Code 2010.

400 COMPARISON OF THE PREDICTIVE PERFORMANCE OF THE DEVELOPED MODELS

401 In this section the predictive performance of the refined and simplified models (*The-refin*, *The-simpl*)
402 developed in the present work for the evaluation of the punching failure load of SFRC flat slabs is compared
403 to the one of the following models found in the literature: Narayanan and Darwish (1987), Shaaban and
404 Gesund (1994), Harajli *et al.* (1995), Holanda (2002), Choi *et al.* (2007), Muttoni and Ruiz (2010) and
405 Higashiyama *et al.* (2011). The formulation of these models is presented in Moraes Neto (2013) and Moraes-
406 Neto *et al.* (2012). Like in a previous Section, the predictive performance of the models was based on the
407 evaluation of the $\lambda = V_{exp}/V_{the}$ parameter and on the analysis of λ according to the modified version of the
408 DPC, where the V_{exp} is the punching failure load of the slabs collected in the database described in Section
409 “Database (DB)”. The models in analysis are designated as *MODi* ($i=1$ up to 9), with the corresponding
410 formulation assigned in the footnote of Table 5 and in the caption of Figure 7. The box plot diagram in
411 Figure 7 graphically depicts the statistical five-number summary, consisting of the minimum and maximum
412 values, and the lower, median and upper quartiles of λ for each model. From the analysis of Figure 7 and the
413 values included in Table 5 it can be concluded that the proposed models, together with the model of Muttoni
414 and Ruiz (2010), are those that assure values of λ closer to the unity with the lowest COV. However, the
415 models proposed in the present work provided the smallest total penalties, with the largest number of
416 predictions in the appropriate safety interval.

417

418 CONCLUSIONS

419 In the present paper a model was proposed to predict the punching failure load of steel fibre reinforced
420 concrete (SFRC) slabs centrally loaded (V_R). This model is supported on the assumption that $V_R = V_{R,c} + V_{R,f}$,
421 where $V_{R,c}$ and $V_{R,f}$ is the contribution of concrete and fibre reinforcement for the punching resistance,
422 respectively. To determine the best available formulation for the prediction of $V_{R,c}$, the predictive
423 performance of models proposed by ACI 318, CEB-FIP Model Code 1990, EC2 and CEB-FIP Model Code
424 2010 was assessed by estimating the punching tests results collected in a database (DB) built for this
425 purpose. From this study it was concluded that CEB-FIP Model Code 2010 evaluates more accurately the
426 concrete contribution for the punching resistance of RC slabs, and consequently it was selected to be

427 combined with the formulation developed for the prediction of the punching resistance of SFRC slabs. This
428 formulation is supported in the critical shear crack theory, and integrates a stress-crack width relationship
429 ($\sigma_f(w)$) for modelling the contribution of fibre reinforcement mechanisms. The $\sigma_f(w)$ was determined
430 according to the recommendations of CEB-FIP Model Code 2010 for the characterisation of the post-
431 cracking flexural tensile behaviour of FRC. The proposed model has two levels of sophistication, one of
432 more laborious calculus, and the other with a simpler way of obtaining the $V_{R,f}$.
433 The predictive performance of these two versions of the developed model was appraised by simulating the
434 punching tests composing the DB. Both versions of the model have predicted with high accuracy the failure
435 load of the punching tests of the DB, and assured better and safer predictions than the ones obtained with
436 available models for the evaluation of the punching failure load of SFRC slabs.

437

438 **ACKNOWLEDGEMENTS**

439 The study presented in this paper is a part of the research project titled “*SlabSys-HFRC - Flat slabs for multi-*
440 *storey buildings using hybrid reinforced self-compacting concrete: an innovative structural system*”, with
441 reference number of PTDC/ECM/120394/2010. The first author acknowledges the support provided by the
442 CAPES and CNPq grant, and the grant provided by the project *SlabSys*.

443

444 **REFERENCES**

- 445 ACI 318. Building Code Requirements for Structural Concrete, *American Concrete Institute*, Farmington
446 Hills, Michigan, 2008.
- 447 Barros, J.A.O.; Cunha, V.M.C.F.; Ribeiro, A.F.; Antunes, J.A.B. “Post-Cracking Behaviour of Steel Fibre
448 Reinforced Concrete”. *RILEM Materials and Structures Journal*, 38(275), pp. 47-56, 2005.
- 449 Barros, J.A.O.; Salehian, H.; Pires, N.M.M.A; Gonçalves, D.M.F. “Design and testing elevated steel fibre
450 reinforced self-compacting concrete slabs”. *BEFIB2012–Fibre reinforced concrete*, 2012.
- 451 BS 8110. Structural Use of Concrete. *British Standards Institution*, 1985.
- 452 CEB-FIP. *Model Code 1990*: Final Draft. Bulletin D’Information, n° 203-205, CEB, Lausanne, July 1991.
- 453 CEB-FIP. *Model Code 2010*: Final Draft. Model Code prepared by Special Activity Group 5, Lausanne,
454 September 2011.

455 Choi, K-K.; Taha, M.M.R.; Park, H-G.; Maji, A.K. “Punching shear strength of interior concrete slab-
456 column connections reinforced with steel fibers”. *Cement & Concrete Composites*, 29(5), pp. 409-420, May,
457 2007.

458 Collins, M.P. “Evaluation of shear design procedures for concrete structures”. *A Report prepared for the*
459 *CSA technical committee on reinforced concrete design*, 2001.

460 Cunha, V.M.C.F.; Barros, J.A.O.; Sena-Cruz, J.M. “Pullout behaviour of steel fibres in self-compacting
461 concrete”. *ASCE Materials in Civil Engineering Journal*, 22(1), pp. 1-9, January, 2010.

462 Destrée, X.; Mandl, J. “Steel fibre only reinforced concrete in free suspended elevated slabs: Case studies,
463 design assisted by testing route, comparison to the latest SFRC standard documents”. *Taylor Made Concrete*
464 *Structures – Walraven & Stoelhorst (eds)*, Taylor & Francis Group, pp. 437-443, London, 2008.

465 Destrée, X.; Bissen, A.M.; Bissen, Luxembourg. “Steel-fibre-only reinforced concrete in free suspended
466 elevated slabs”. *Concrete Engineering International*, Spring, pp. 47-49, 2009.

467 Espion, B. “Test report n°33396”, University of Brussels, Belgium, 2004.

468 Eurocode 2. Design of Concrete Structures. Part 1-1: General Rules and Rules for Buildings. *European*
469 *Standard*, 2004.

470 Gardner, N.J.; Huh, J.; Chung, L. “Lessons from the Sampoong department store collapse”. *Cement &*
471 *Concrete Composites*, 24, pp. 523-529, 2002.

472 Guandalini, S. Poinçonnement symétrique des dalles en béton armé. *PhD Thesis* 3380, Ecole Polytechnique
473 Fédérale de Lausanne, Switzerland, 2005. (in French)

474 Harajli, M.H.; Maalouf D.; Khatib H. “Effect of fibres on the punching shear strength of slab-column
475 connections”. *Cement & Concrete Composites*, 17(2), pp. 161-170, 1995.

476 Higashiyama, H.; OTA, A.; Mizukoshi, M. “Design equation for punching shear capacity of SFRC slabs”.
477 *International Journal of Concrete Structures and Materials*, 5(1), pp. 35-42, 2011.

478 Holanda, K.M.A. Analysis of resistant mechanisms and similarities of the addition effect of steel fibers on
479 strength and ductility to both punching shear of flat and the shear of concrete beams. *PhD Thesis*. São
480 Carlos, Brazil, 2002. (in Portuguese)

481 Johansen, K.W. “Yield-line theory”. *Cement and Concrete Association*, 1962.

482 Mandl, J. “Flat slabs made of steel fibre reinforced concrete (SFRC),” *CPI Worldwide*, 1, 2008.

483 Michels, J.; Waldmann, D.; Maas, S.; Zürbes, A. “Steel fibers as only reinforcement for flat slab construction
484 – Experimental investigation and design”. *Construction and Building Materials*, 26(1), pp. 145-155, 2012.

485 Moraes-Neto, B.N.; Barros, J.A.O.; Melo, G.S.S.A. “The predictive performance of design models for the
486 punching resistance of SFRC slabs in inner column loading conditions”. *8th RILEM International symposium
487 on fibre reinforced concrete: challenges and opportunities (BEFIB 2012)*, September, 2012.

488 Moraes Neto, B.N. Punching behaviour of steel fibre reinforced concrete slabs submitted to symmetric
489 loading. PhD in Civil Engineering, Department of Civil and Environmental Engineering, University of
490 Brasília, Brasília, DF, January, 2013. (in Portuguese)

491 Muttoni, A.; Schwartz, J. “Behaviour of Beams and Punching in Slabs without Shear Reinforcement”. *IABSE
492 Colloquium*, 62, pp. 703-708, Zurich, Switzerland, 1991.

493 Muttoni, A. “Punching shear strength of reinforced concrete slabs without transverse reinforcement”. *ACI
494 Structural Journal*, 105(4), pp. 440-450, July/August, 2008.

495 Muttoni, A.; Ruiz, M.F. “The critical shear crack theory as mechanical model for punching shear design and
496 its application to code provisions”. *Fédération Internationale du Béton, Bulletin 57*, Lausanne, Switzerland,
497 pp. 31-60, 2010.

498 Narayanan, R., Darwish, I.Y.S. “Punching Shear Tests on Steel Fibre Reinforced Microconcrete Slabs”,
499 *Magazine of Concrete Research*, 39(138), pp. 42-50, 1987.

500 Sasani, M. and Sagioglu, S. “Progressive collapse of reinforced concrete structures: a multihazard
501 perspective”, *ACI Structural J.*, 105(1), pp. 96-105, 2008.

502 Shaaban, A.M.; Gesund, H. “Punching shear strength of steel fiber reinforced concrete flat plates”. *ACI
503 Structural Journal*, 91(4), pp. 406-414, Jul/Aug, 1994.

504

505

506

507

508

509

510

511

512

513

514

NOTATION

A_0	Horizontal projection of failure surface
A_s	Area of tension reinforcement
A'_s	Area of compression reinforcement
b	Width of a isolated slab element
b_0	Critical perimeter for punching shear (ACI 318 and CEB-FIP Model Code 2010)
b_s	Strip of slab to avalue the bending moment
d	Internal arm of the slab
d_f	Diameter of fibre
d_g	Maximum diameter of the
E	Modulus of elasticity of concrete
E_s	Modulus of elasticity of reinforcement
f_c	Average compressive strength of concrete in cylinder specimens
f_{ct}	Average tensile strength of concrete (Brazilian test)
f_{Fts}	Post-cracking strength for serviceability crack opening
f_{Ftu}	Post-cracking strength for ultimate crack opening
f_{Ri}	Residual flexural tensile strength of fibre reinforced concrete corresponding to CMOD _i
f_{yd}	Design yield strength of reinforcement
F_s	Internal compressive force of tensile reinforcement
F'_s	Internal compressive force of compressive reinforcement
h	Slab thickness
I_1	Second moment of area of cracked concrete cross-section
k, ζ	Size effect parameter
k_{dg}	Aggregate interlock parameter
k_ψ	Rotation of the slab parameter
l_f	Length of fibre
L	Span of slab
m_R	Resisting bending moment (plastic bending moment)
m_{sd}	Actuating bending moment
r_0	Radius of the critical shear crack
r_c	Radius of a circular column
r_q	Radius of the load introduction at the perimeter
r_s	Radius of circular isolated slab element
u_1	Critical perimeter for punching shear (EC2 and CEB-FIP Model Code 1990)
V	Shear force
V_f	Fibre volume percentage
$V_{R,cd}$	Design concrete contribution to punching shear strength
$V_{R,d}$	Design punching shear strength
$V_{R,fd}$	Design fibre contribution to punching shear strength
$V_{R,sd}$	Design shear reinforcement contribution to punching shear strength
$V_{s,d}$	Actuating shear force
w	Shear crack opening
w_u	Maximum acceptable crack width imposed by design conditions
x	Neutral axis of slab

α_s	Parameter for columns located in the interior of the building
β	Efficiency factor of the bending reinforcement for stiffness calculation
β_c	Ratio between the larger and the smaller edge of the column's cross section
χ_{ts}	Tension stiffening parameter
ε_c	Concrete strain
ε_{cu}	Ultimate strain of concrete in compression zone
ε_{fu}	Ultimate strain of fibre in tensile zone
ε_s	Strain of steel reinforcement in tensile zone
ε_{su}	Ultimate strain of steel reinforcement in tensile zone
ε'_s	Compressive steel reinforcement strain
$\varepsilon_{i,bot}$	Concrete tensile strain at the bottom surface of the slab
$v_{N,d}$	Design nominal shear stress
$v_{R,d}$	Design shear strength
τ_f	Average interracial bond strength of fibre matrix
ρ	Tensile reinforcement ratio
σ	Stress
ψ	Rotation of slab

515

516
517
518

LIST OF TABLE CAPTIONS

- 519 Table 1. Modified version of the *Demerit Points Classification* (DPC).
520 Table 2. Predictive performance of the design models according to the modified version of the DPC.
521 Table 3. Predictive performance of Eqs. (20) and (21) in the context of the modified version of the DPC.
522 Table 4. Performance of models for the prediction of the punching failure load of SFRC flat slabs according to the
523 modified version of the DPC.
524 Table 5. Performance of several models to predict V_{exp} : classification of the models according to the modified version of
525 the DPC
526

Table 1. Modified version of the *Demerit Points Classification* (DPC).

$\lambda = V_{exp}/V_{the}$	Classification	Penalty (PEN)
< 0.50	Extremely Dangerous	10
[0.50-0.85[Dangerous	5
[0.85-1.15[Appropriate Safety	0
[1.15-2.0[Conservative	1
≥ 2.0	Extremely Conservative	2

527
528
529
530
531
532
533
534
535
536
537
538
539
540
541

542

Table 2. Predictive performance of the design models according to the modified version of the DPC.

$\lambda = V_{exp}/V_{the}$		< 0.50	[0.50-0.85[[0.85-1.15[[1.15-2.00[≥ 2.00	Total PEN	AVG	STD	COV (%)
MOD1	N° samples	0	3	3	18	0	24	1.28	0.32	25.28
	PEN	0	15	0	18	0	33			
MOD2	N° samples	0	7	14	3	0	24	0.95	0.20	20.91
	PEN	0	35	0	3	0	38			
MOD3	N° samples	0	1	15	8	0	24	1.16	0.25	21.30
	PEN	0	5	0	8	0	13			
MOD4	N° samples	0	2	21	1	0	24	1.01	0.09	9.34
	PEN	0	10	0	1	0	11			

MOD1=ACI 318, MOD2 =CEB-FIP Model Code 1990, MOD3=EC2, MOD4=CEB-FIP Model Code 2010.

543

544

545

546

547

548

549

550

551

552

553

554

555

556

557

558

559

560

561

562

563

564

Table 3. Predictive performance of Eqs. (20) and (21) in the context of the modified version of the DPC.

f_{Ri}	f_{R1}		f_{R3}	
$\lambda_i = f_{Ri,exp}/f_{Ri,the}$	N° samples	PEN	N° samples	PEN
< 0.50	0	0	1	10
[0.50-0.85[4	20	7	35
[0.85-1.15[17	0	18	0
[1.15-2.00[43	43	38	38
≥ 2.00	5	10	5	10
Total PEN	69	73	69	93
Statistical resume				
f_{Ri}	f_{R1}		f_{R3}	
Average (AVG)	1.37		1.32	
STD	0.38		0.48	
COV (%)	27.88		36.08	

565

566

567

568

569

570

571

572

573

574

575

576

577

578

579

580

581

582

583

584

Table 4. Performance of models for the prediction of the punching failure load of SFRC flat slabs according to the modified version of the DPC.

Models	<i>The-refin</i>		<i>The-simpl</i>		CEB-FIP Model Code 2010	
$\lambda = V_{exp} / V_{the}$	N° samples	PEN	N° samples	PEN	N° samples	PEN
< 0.50	0	0	0	0	2	20
[0.50-0.85[6	30	5	25	39	195
[0.85-1.15[43	0	42	0	9	0
[1.15-2.00[1	1	3	3	0	0
≥ 2.00	0	0	0	0	0	0
Total PEN	50	31	50	28	50	215
Statistical resume						
Models	<i>The-refin</i>		<i>The-simpl</i>		CEB-FIP Model Code2010	
Average (AVG)	0.97		0.98		0.73	
STD	0.11		0.11		0.13	
COV (%)	11.38		11.17		17.48	

585

586

587

588

589

590

591

592

593

594

595

596

597

598

599

600

601

602

Table 5. Performance of several models to predict V_{exp} : classification of the models according to the modified version of the DPC

$\lambda = V_{exp} / V_{the}$		< 0.50	[0.50-0.85[[0.85-1.15[[1.15-2.00[≥ 2.00	Total PEN	AVG	STD	COV (%)
MOD1	N° samples	0	21	21	8	0	50	0.92	0.23	25.29
	PEN	0	105	0	8	0	113			
MOD2	N° samples	0	2	18	29	1	50	1.24	0.26	20.89
	PEN	0	10	0	29	2	41			
MOD3	N° samples	0	5	18	20	7	50	1.42	0.62	43.38
	PEN	0	25	0	20	14	59			
MOD4	N° samples	0	0	8	42	0	50	1.32	0.20	15.47
	PEN	0	0	0	42	0	42			
MOD5	N° samples	0	6	17	27	0	50	1.20	0.29	24.03
	PEN	0	30	0	27	0	57			
MOD6	N° samples	0	6	37	7	0	50	0.99	0.13	13.26
	PEN	0	30	0	7	0	37			
MOD7	N° samples	0	20	24	6	0	50	0.92	0.18	19.45
	PEN	0	100	0	6	0	106			
MOD8	N° samples	0	6	43	1	0	50	0.97	0.11	11.38
	PEN	0	30	0	1	0	31			
MOD9	N° samples	0	5	42	3	0	50	0.98	0.11	11.17
	PEN	0	25	0	3	0	28			

MOD1= Narayanan and Darwish (1987); MOD2= Shaaban and Gesund (1994); MOD3= Harajli *et al.* (1995); MOD4= Holanda (2002); MOD5= Choi *et al.* (2007); MOD6= Muttoni and Ruiz (2010); MOD7= Higashiyama *et al.* (2011); MOD8=*The-refin*; MOD9=*The-simpl*

604

605

606

607

608

609

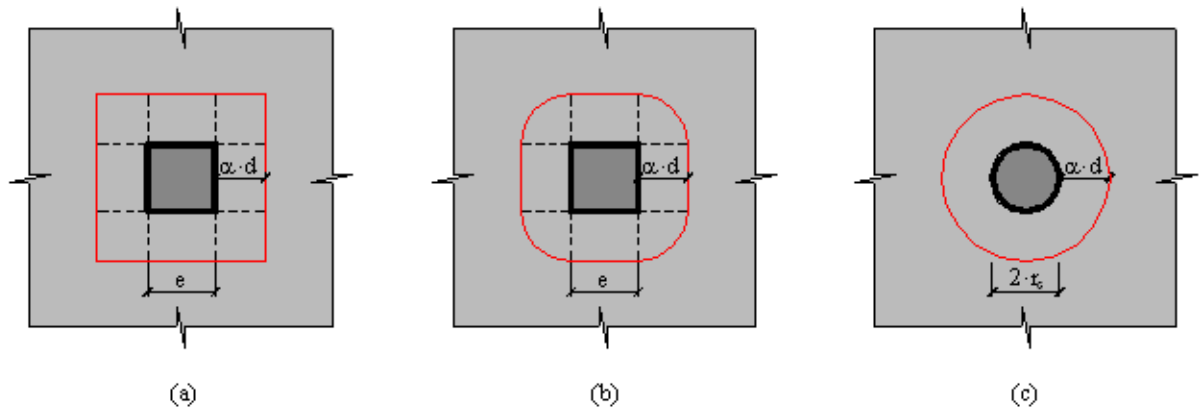


Figure 1. Punching failure perimeter adopted for the evaluation of the punching resistance when columns have: (a) and (b) square cross section, (c) circular cross section.

610

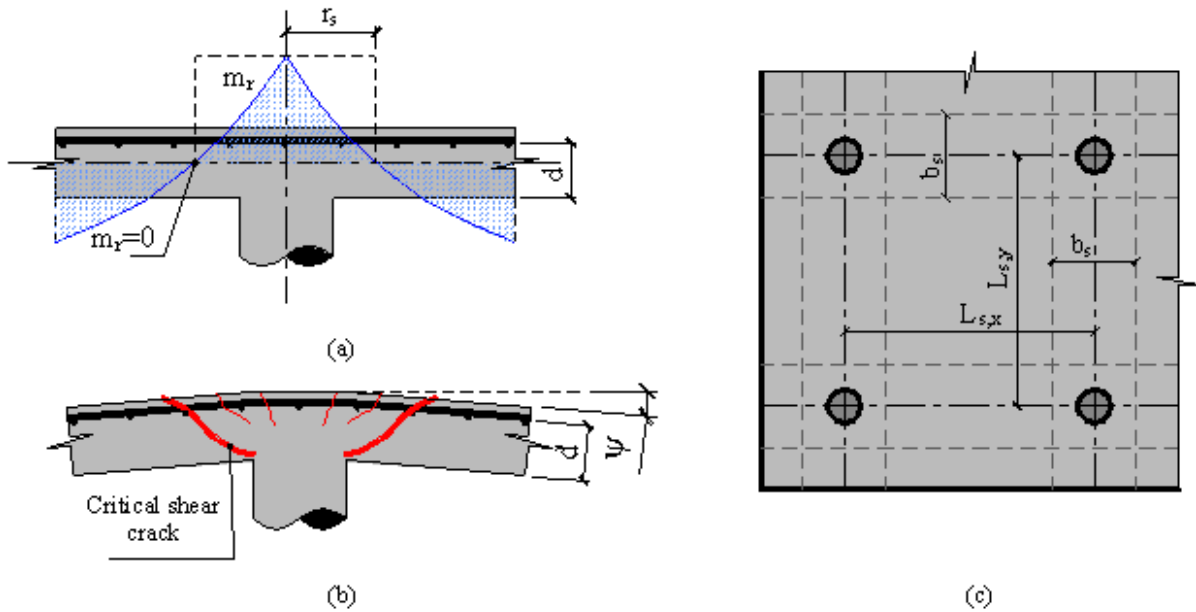


Figure 2. Characteristics of the slab: (a) Distribution of the radial bending moment, (b) Slab's rotation at failure (c) Representation of the slab's spans and width of slab's strips.

611

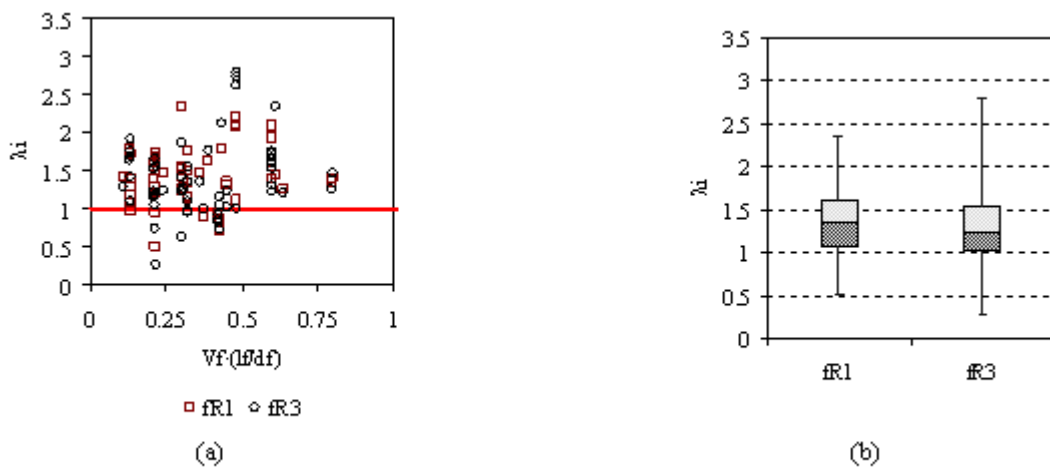


Figure 3. Predictive performance of Eqs. (20) and (21).

612

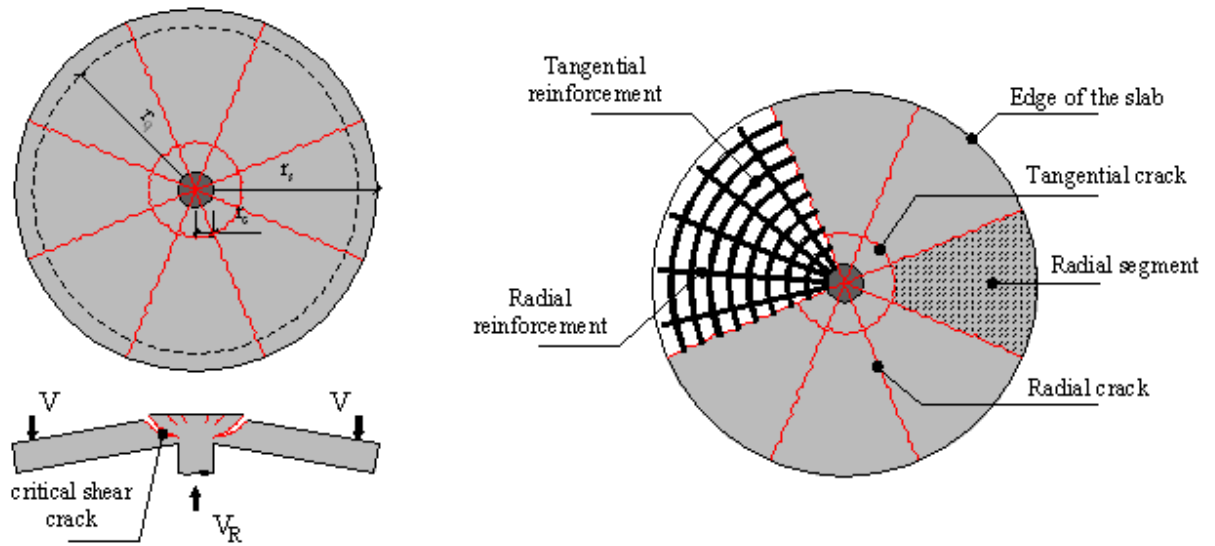


Figure 4. RC slab with axisymmetric structural conditions, crack pattern at ultimate limit state and reinforcement arrangement.

613

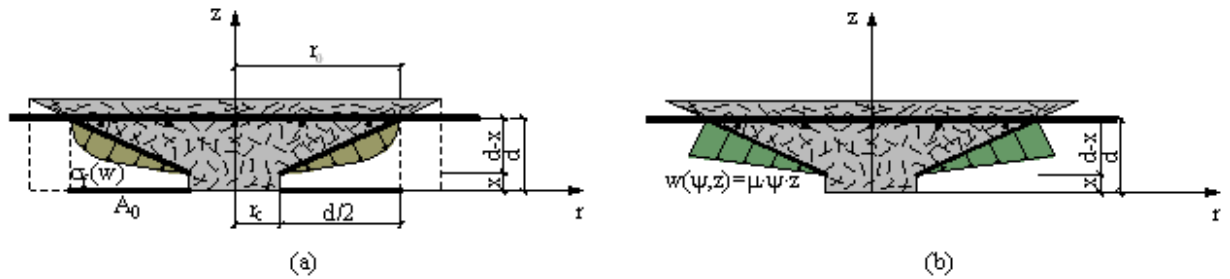


Figure 5. Contribution of fibre reinforcement mechanisms for the punching resistance: (a) stress distribution and (b) crack opening idealization.

614

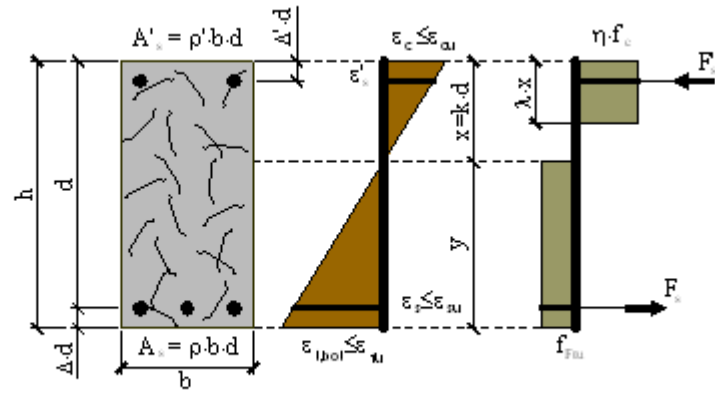


Figure 6. Adopted approach to evaluate x and m_R (adapted from the CEB-FIP Model Code 2010 [8]).

615

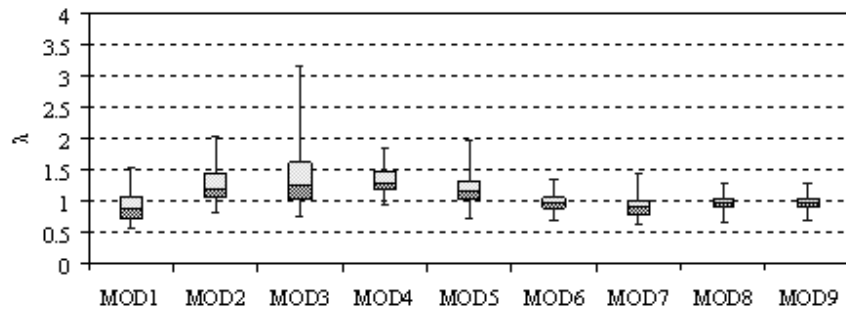


Figure 7. Comparison of the predictive performance of available and proposed models.

MOD1= Narayanan and Darwish [13]; MOD2= Shaaban and Gesund [27]; MOD3= Harajli *et al.* [14]; MOD4= Holanda [28]; MOD5= Choi *et al.* [23]; MOD6= Muttoni and Ruiz [15]; MOD7= Higashiyama *et al.* [24]; MOD8= *The-refin*; MOD9= *The-simpl*

616

617

618

619

620

621

622